Water Air Soil Pollut (2011) 217:221–232
DOI 10.1007/s11270-010-0581-z

Seasonal Variation of Mercury Associated with Different Phytoplankton Size Fractions in Lahontan Reservoir, Nevada

Rosemary W. H. Carroll · Jeramie Memmott · John J. Warwick · Christian H. Fritsen · Jean-Claude J. Bonzongo · Kumud Acharya

Received: 27 December 2009 / Accepted: 28 July 2010 / Published online: 14 August 2010

Abstract Sampling is conducted during 2006 in Lahontan Reservoir, Nevada to investigate seasonal variation of total mercury (THg) and methylmercury (MeHg) partitioning in different phytoplankton size fractions as a function of point source (fluvial) mercury (Hg) loads, reservoir residence time, and algal growth. Carson River Hg inputs into the reservoir are extremely dynamic with spring loads two orders of magnitude larger than summer loads. Chlorophyll *a* measurements show two periods of algal growth. A small amount of algal growth occurs March to May. A second more substantial bloom occurs in the late summer, which is dominated by large, filamentous algae. THg concentrations (C_b) and partitioning coefficients (K_d) in total suspended particulate matter (SPM) are highest when fluvial inputs of Hg-contaminated sediment are large and are not necessarily associated with living biomass. However, MeHg K_d in the small size fraction is indirectly related to fluvial loads and more strongly associated with living biomass in the later portion of the summer when algal growth occurs and reservoir residence times are longer. Data suggest size distinction is important to MeHg partitioning in the reservoir. Lumping all sizes into a single SPM sample will bias the analysis toward low MeHg C_b and low MeHg K_d in late summer when *Aphanizomenon flos-aquae* dominates the phytoplankton assemblage.

Keywords Mercury · Partition coefficient · Phytoplankton · Eutrophic reservoir

R. W. H. Carroll (✉) · J. J. Warwick
Division of Hydrologic Sciences, Desert Research Institute,
2215 Raggio Parkway,
Reno, NV 89512, USA
e-mail: Rosemary.Carroll@dri.edu

J. J. Warwick
e-mail: John.Warwick@dri.edu

J. Memmott · C. H. Fritsen
Division of Earth and Ecosystem Sciences,
Desert Research Institute,
2215 Raggio Parkway,
Reno, NV 89512, USA

J. Memmott
e-mail: Jeramie.Memmott@dri.edu

C. H. Fritsen
e-mail: Chris.Fritsen@dri.edu

J.-C. J. Bonzongo
Environmental Engineering Sciences,
University of Florida,
320 Black Hall,
Gainesville, FL 32611-6450, USA
e-mail: bonzongo@ufl.edu

K. Acharya
Division of Hydrologic Sciences,
755 E. Flamingo Road,
Las Vegas, NV 89119, USA
e-mail: Kumud.Acharya@dri.edu

1 Introduction

Trophic enrichment of mercury (Hg) is relatively uniform across a range of food webs (benthic versus pelagic versus stream), ecological settings (marine versus freshwater), and exposure conditions (point source versus atmospheric deposition) (Kidd et al. 1995; Pickhardt et al. 2005; Stewart et al. 2008; Chasar et al. 2009). Since enrichment factors between trophic levels are fairly consistent, difference in top predator fish can often be attributed to differences in Hg availability and accumulation efficiency at the base of the food web (Stewart et al. 2008; Chasar et al. 2009). Stewart et al. (2008) found pelagic systems to be more effective at accumulating Hg compared to benthic systems. Phytoplankton represent the base of pelagic food webs and have been found to bioaccumulate Hg up to 10^5 times more than successive trophic transfers (Watras et al. 1998; Moye et al. 2002; Pickhardt and Fisher 2007). Therefore, small changes in phytoplankton bioaccumulation may have significant implications on overall Hg bioaccumulation in the system as a whole.

The inverse relationship between algal growth rate and bioaccumulation presented by Mason et al. (1996) helps explain growth dilution and is supported by several studies which found that higher phytoplankton densities and/or growth rates resulted in less Hg accumulation in both plankton communities as well as at higher trophic levels (Karimi et al. 2007; Chen and Folt 2005; Pickhardt et al. 2005; Pickhardt and Fisher 2007). Algal bloom dilution, however, can occur for different reasons: rapid growth such that the growth rate becomes larger than the rate of Hg sequestration in phytoplankton, preferential partitioning of Hg to non-living particles (Laurier et al. 2003; Schāfer et al. 2006; Luengen and Flegal 2009), or limited supply of dissolved Hg species such that uptake depletes water column concentrations during early portions of a bloom (Luengen and Flegal 2009).

Size of the algae, as depicted by Mason et al. (1996), may also influence Hg uptake efficiency. Those with greater surface area to volume are expected to accumulate Hg more rapidly. Work by Pickhardt and Fisher (2007) found this to be true for MeHg; however, MeHg uptake was not established as a passive, diffusional process. It is believed to be metabolically controlled, as exemplified by much larger accumulation of MeHg in live versus dead diatoms. Moye et al. (2002) also found MeHg uptake dependent on active cellular metabolism, but unlike Pickhardt and Fisher (2007), they found MeHg uptake efficiency to be not always size dependent. Instead, species-specific membrane permeability was speculated as an important parameter in describing uptake efficiency.

In contrast to MeHg uptake, Pickhardt and Fisher (2007) found inorganic Hg insensitive to cell size. They suggest that accumulation of inorganic Hg is a function of binding to the ubiquitous organic film found on all particles, living and non-living. Likewise, Luengen and Flegal (2009) show that total Hg (THg), a surrogate for inorganic Hg, preferentially binds to non-living matter (material from broken and decaying cells or organically coated clay particles) with phytoplankton THg concentrations relatively low compared to other types of suspended material.

Given the potential importance of Hg bioaccumulation through the pelagic pathway, this study is focused on relative uptake of THg and MeHg in different size fractions of phytoplankton. The system examined is a eutrophic reservoir in northern Nevada impacted by historic mining of gold and silver through Hg amalgamation techniques. Hg loads into the reservoir are highly dynamic. It is hypothesized that phytoplankton abundance along with the size of the phytoplankton and the timing of Hg loads may impact Hg uptake efficiency into the lower food web.

2 Site Description

The Carson River–Lahontan Reservoir system (CRLR) in west-central Nevada (Fig. 1) is listed by the United States Environmental Protection Agency (US EPA) as a Superfund site due to its contamination with Hg derived from mining of the Comstock Lode in the later portion of the nineteenth century (NVD980813646). Lahontan Reservoir was constructed in 1915 and is used to irrigate fields in Lahontan Valley and is managed as a warm water fishery. Lahontan Reservoir consists of three distinct basins with water from the Carson River entering the south basin and moving northward through the middle basin and into the north basin. The north basin terminates at Lahontan Dam. Narrow channels connect each of the basins and are marked as Fisherman's Point (FPO), which connects the south

Fig. 1 Lahontan Reservoir with Fisherman's Point (*FPO*) sampling site marked. The Carson River enters the southern basin of the reservoir. The USGS sampling site at Weeks Bridge is located 8 km upstream from the Carson River's delta. *Upper inset* shows location of the Carson River—Lahontan Reservoir (CRLR) watershed with respect to the western USA

and middle basins, and the Narrows, which connects the middle and north basins. The dominant source of unfiltered and dissolved THg as well as unfiltered and dissolved MeHg into the reservoir is the Carson River (Gandhi et al. 2007; Diamond et al. 2000). The United States Geological Survey (USGS) water column THg and MeHg concentrations (C_w) collected 8 km upstream from the river's delta at Weeks Bridge (USGS site 10312020) acts as a surrogate for fluvial concentrations entering the reservoir. Water column concentrations collected at Weeks Bridge are compared to those collected at FPO to assess the importance of seasonal inputs from the Carson River.

Phytoplankton provide most of the primary production in Lahontan Reservoir due to a limited littoral zone and drastic water level fluctuations in the reservoir. Cooper et al. (1983) observed that 99% of the phytoplankton sampled in the reservoir is Cyanophyta, with *Aphanizomenon flos-aquae* dominating the assemblage. Cyanophyta peak in the hot summer months (10^6 cells/mL) with the magnitude and duration of the bloom increasing from the south basin to the north basin. These large, filamentous cynobacteria decrease to negligible population levels (<1 cell/mL) in the winter months in all three reservoir basins. Diatoms, on the other hand, have concentrations several orders of magnitude lower than cyanobacteria but maintain relatively high populations in the fall and winter months (100–200 cells/mL). Populations of diatoms are lowest in the north basin of the reservoir and highest in the middle and south basins.

3 Methods

3.1 Reservoir Water Column Sampling

Samples for water column chemistry and phytoplankton biomass are obtained at FPO. FPO is chosen for hydrologic reasons. Its location represents a compro-

mise of being close enough to the river's delta to preserve a well-defined mercury pulse entering the reservoir's south basin, but far enough from the river's delta to reduce the risk of the delta migrating northward past the sampling location during reservoir drawdown in the summer months. The choice of FPO minimizes sampling logistics because of its narrow cross section (approx. 100 m) and its accessibility by boat. Water column samples are collected every 6 weeks beginning early March 2006 to capture peak spring runoff from the Carson River. Sampling continues into late September to catch a possible secondary peak of smaller phytoplankton and to observe potential influences of internal cycling of Hg on accumulation in phytoplankton (e.g., diffusion from the reservoir's benthic sediments, water column methylation of inorganic Hg, sorption kinetics that make previously biologically unavailable Hg more readily available for biologic uptake).

Vertical measurements of temperature, pH, oxidation-reduction potential, specific conductivity, in vivo fluorescence, photosynthetically active radiation, turbidity, and dissolved oxygen are obtained with a YSI 6600 probe at three equidistant locations across the FPO cross section for use in later modeling studies. Maximum depth of the reservoir at FPO is approximately 13 m along the right bank and at the center profile but only 2.5 m along the left bank. During all sampling surveys, water is collected from a total of ten discrete locations with sample depths dependent on reservoir stage. Figure 2 is a schematic of the FPO cross section with discrete sample locations marked.

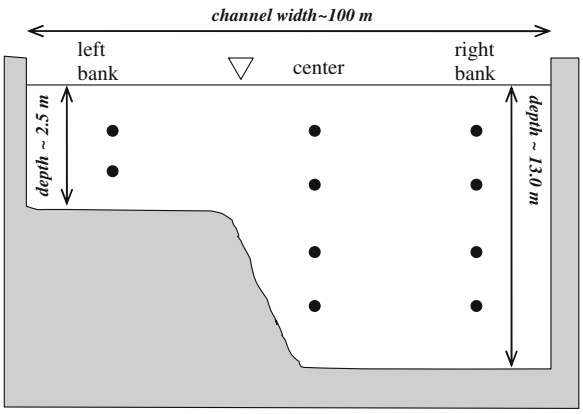

Fig. 2 Schematic of FPO cross section with discrete water column sampling sites marked as *black circles*

Discrete water samples are collected using a Teflon tube and peristaltic pump. Those collected for chlorophyll *a* (Chl*a*), suspended particulate matter (SPM), and SPM-associated Hg concentrations (algal material not separated from inorganic SPM in the filtering process) are stored in opaque, high-density polyethylene (HDPE) 1-L bottles and transported on ice back to the Desert Research Institute (DRI) analytical facilities. At DRI, all ten discrete samples are combined in a 14-L, Teflon, USGS Water Quality Modified Churn Splitter to form composite samples for analysis. The use of the churn splitter is done to minimize the cost associated with Hg analysis while maintaining a representative weighted volume sample for the site. Additional water is collected at each of the ten discrete sample locations and placed in 1-L, opaque, HDPE bottles to measure Chl*a*, SPM, and a partial suite of nutrients to compare spatial variability to composite samples. Teflon tubing, HDPE bottles, and the churn are all pre-cleaned with 10% HNO_3 for 48 or more hours and thoroughly rinsed with milliQ. Tubing and bottles are also thoroughly rinsed with reservoir water prior to sample collection. Water column Hg samples are collected using equivalent quantities from each discrete location and combined in an acid-washed Teflon bottle using the clean hands-dirty hands protocol (US EPA 1996).

Filtering for SPM THg and MeHg analysis and subsequent freezing at −80°C is done within 3 to 8 h after collection with further analysis done within 2 weeks. Standard filtration procedures are conducted with glass fiber filters (GF/F, 0.7 μm). Chl*a* is determined fluorometrically (Welschmeyer 1994) while SPM mass is determined using method 2540D. SPM is dried at 103°C to 105°C as described in Clesceri et al. (1998). Total SPM is obtained by pumping a sample directly onto a GF/F filter. The fraction of SPM smaller than (<) 35 μm is obtained by passing the sample through a 35-μm Nitex® net prior to pumping onto the GF/F. The fraction greater than (>) 35 μm is not measured directly, but inferred from the difference between the total sample and that less than 35 μm.

3.2 Mercury Analysis

Hg analysis requires water sample aliquots to be filtered (0.45 μm) into acid pre-cleaned Teflon bottles, and both filtered and unfiltered fractions are acidified with ultra-pure HCl at a final concentration

of 1% (*v*/*v*). Samples are then kept refrigerated at 4°C until analysis. THg concentrations are determined after subjecting water samples to $BrCl/SnCl_2$, followed by gas-phase purging with Hg-free N_2 and trapping of Hg^0 onto gold-coated sand. The Hg^0 is then thermally desorbed from the gold-trap and released into an Hg-free helium stream and quantified by cold vapor atomic fluorescence spectrometry (CV-AFS). MeHg is first separated from its original matrix by extraction in an organic solvent (Bloom 1989; Horvat et al. 1993) and then ethylated using sodium tetraethylborate (Bloom 1989), followed by CV-AFS detection after GC separation and thermal decomposition of alkyl-Hg compounds. Quality assurance/quality control procedures included instrument calibration using standard solutions, certified reference materials, duplicate analyses, and reagent blanks. The detection limit, defined as three times the standard deviation of purged blanks, is 0.06 and 0.01 ng/L for Hg and MeHg, respectively. The percent recovery on spiked samples averaged 98±5% (n=7) for THg and 90±8% (n=8) for MeHg.

Hg analyses for total SPM and that <35 μm on a wet weight basis are done independently. THg in SPM is determined after digestion in a volumetric flask with a 7:3 mixture of concentrated HNO_3/H_2SO_4. Aliquots from the digestate are then analyzed by $SnCl_2$-reduction technique with detection by CV-AFS. MeHg is determined using a method adapted from Bloom (1989), where it is first released from the sample matrix by solvent extraction, followed by ethylation, Tenax® trapping, GC separation, thermodecomposition, and detection by CV-AFS. For both THg and MeHg, in addition to reagent blanks and liquid standard solutions, a certified reference material (IAEA-405, estuarine sediments containing an average of 0.81 mg/kg of THg and 5.49 ng/g of MeHg) was run with all digestions/analyses. The percent recovery on the IAEA-405 averaged 95±11% (n=10) and 93±8% (n=10) for THg and MeHg, respectively. Details regarding analytical procedures have been described elsewhere (e.g., Warner et al. 2003, 2005; Bonzongo et al 2006; Donkor et al. 2005, 2006; Byrne et al. 2009; Cohen et al. 2009).

3.3 Data Analysis

SPM, Chl*a* as well as SPM THg and SPM MeHg concentrations for the total fraction and that <35 μm are normalized by the volume of composite reservoir water used in the filtering process to obtain mass per unit volume of reservoir water (micrograms per liter). Samples of total SPM MeHg collected in June, August, and September fall below the detection limit (<0.001 ng/filter). These samples are assigned detection limit concentrations for discussion purposes. THg and MeHg associated with SPM are further normalized by the mass of SPM to produce mass-specific mercury concentrations (C_b, microgram per gram).

The particulate/dissolved partitioning coefficient, K_d (liter per kilogram), is computed as,

$$K_d = \log\left(\frac{C_b}{C_w^d}\right)$$

where C_w^d is the dissolved water column concentration (milligram per liter). K_d defines the partition coefficient, as opposed to the bioaccumulation factor, because algal material is not separated from inorganic suspended material in the filtering process.

Error in measurements propagates through the calculation of C_b and K_d. Assigned error to C_w^d is the observed standard deviation in replicate samples. Error in SPM mass measurements is determined as the maximum error to rectify mass balance calculations. Mass balance errors are larger than observed variability in duplicate samples and deemed the more conservative approach. Specifically, total SPM is measured less than its subset (SPM<35 μm) on two occasions (error equal to 7.8).

4 Results

4.1 Water Column Concentrations and Loads into the Reservoir

Water column concentrations collected by the USGS at Weeks Bridge (Fig. 3a) are compared to water quality data collected at FPO (Fig. 3b) from March to September, 2006. Estimated fluvial loads (W) into the reservoir and residence time (τ) of water moving through the south basin are provided in Fig. 3c and d, respectively. Concentrations of unfiltered THg at Weeks Bridge surpass 10 μg/L during the spring runoff event reflecting bank erosion of contaminated sediments. Concentrations decrease by more than two orders of magnitude during the late summer. Concentrations of unfiltered THg at FPO also peak during

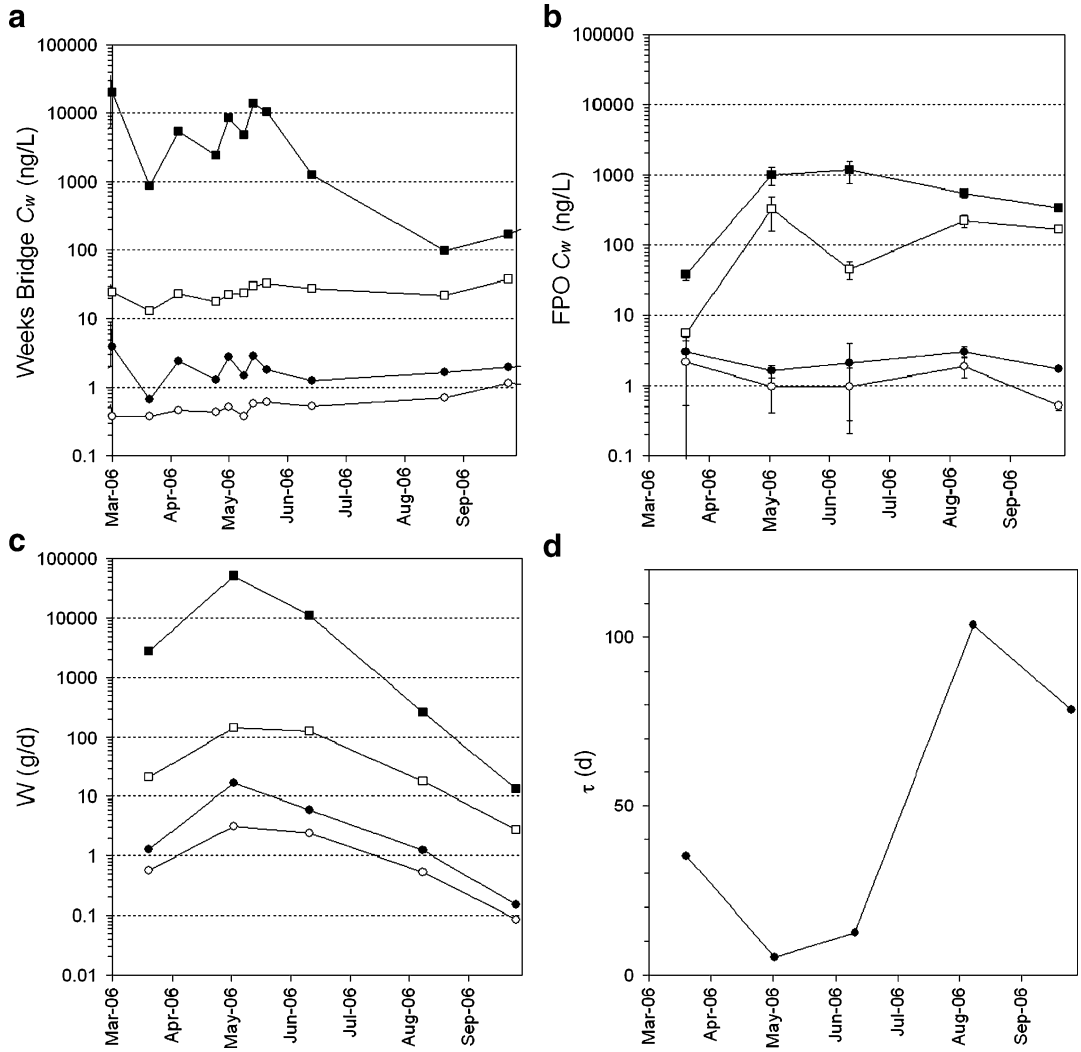

Fig. 3 **a** Water column concentrations (C_w) collected at Weeks Bridge by the USGS and **b** at FPO for this study. *Error bars* at FPO represent one standard deviation of the mean. **c** Loads (W) computed at Weeks Bridge and **d** computed residence time (τ, days) in the reservoir's south basin. *Symbols* represent unfiltered THg (*filled square*), DHg (*unfilled square*), unfiltered MeHg (*filled circle*), and DMeHg (*unfilled circle*)

spring runoff and then decline slowly as the pulse of particle bound THg is attenuated in the reservoir's south basin as water residence time increases. Concentrations of dissolved Hg (DHg) are higher at FPO compared to Weeks Bridge for all sampling dates except March, implying that either DHg originating from the lower section of the Carson River (i.e., below Weeks Bridge) or diffusion from reservoir benthic sediments may be important mechanisms for DHg loading into the reservoir. At FPO, dissolved MeHg (DMeHg) concentrations are relatively constant throughout the sampling period with DMeHg measured between 0.5 and 2.1 ng/L. DMeHg concentrations at FPO are larger than concentrations at Weeks Bridge only in August, implying that, other than late summer, internal loading of DMeHg from reservoir bottom sediments may not be significant compared to point loads from the Carson River.

Loads are calculated as the product of observed concentrations at Weeks Bridge and discharge estimated at the river's delta (entrance to the reservoir's south basin) using a modified version of the US EPA hydrodynamic code RIVMOD (Hosseinipour and Martin 1990), a tool developed for the CRLR system

(Carroll et al. 2000, 2004; Warwick and Heim 1995). Peak loads from the Carson River occur during spring runoff, with unfiltered THg in excess of 50 kg/day. Carson River loads entering the reservoir then diminished by approximately two orders of magnitude for all constituents sampled. The residence time (τ) for water moving through the southern basin of the reservoir is also computed using the CRLR model. Residence time is determined as the quotient of water volume divided by the flow rate (done for individual model segments and summed) with calculations accounting for delta migration as a result of fluctuating reservoir level. Estimated residence times for days when samples are collected at FPO range from 5 days in May to 104 days in August.

4.2 THg and MeHg Associated with Phytoplankton

Chl*a* values for phytoplankton <35 μm range between 1.8 and 8.6 μg/L during the sampling period. Small sized phytoplankton are highest in the late fall and at a minimum biomass during mid-June (Fig. 4). Chl*a* values for the entire assemblage are more dynamic, with Chl*a* >35 μm represented as the difference between the two curves in Fig. 4. Phytoplankton >35 μm has two growth periods. A small increase in biomass occurs between March and May (0.6 to 2.5 μg/L), followed by a decrease in June to nearly 0 μg/L. Larger phytoplankton then grow at a substantial rate during the second half of the summer (up to 24 μg/L), with a subsequent decline witnessed by the end of September (8 μg/L). The percentage (φ) of Chl*a* in the SPM sample mimics Chl*a* concentrations and ranges from 0.008% to 0.2% with minimum living biomass found in June and maximum percentages found in August (for total SPM) and September (for SPM <35 μm). While the percentage of living biomass is small at FPO, it is comparable to Camp Far West Reservoir, located in the western foothills of the Sierra Nevada in California, where φ ranges from 0.02% to 0.39% and SPM MeHg is used to assess accumulation at the base of the pelagic food web (Stewart et al. 2008).

THg C_b (Fig. 5a) for total SPM shows a substantial increase (6 to 51 μg/g) in May when SPM peaks. This

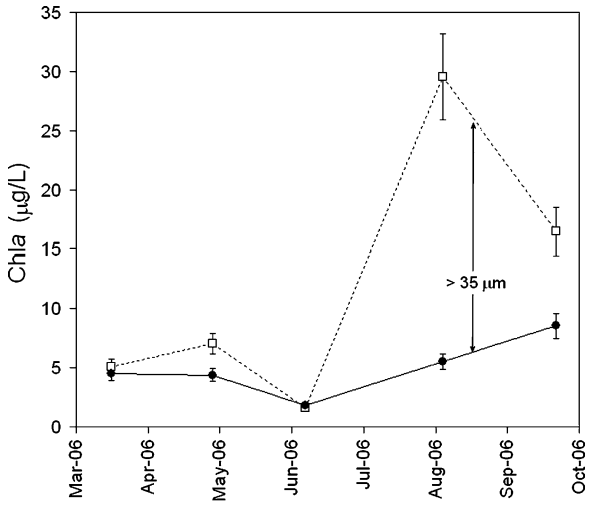

Fig. 4 Chl*a* concentrations in micrograms per liter for phytoplankton <35 μm (*filled circle*) and total phytoplankton (*unfilled square*). Chl*a* >35 μm is the difference between the two curves

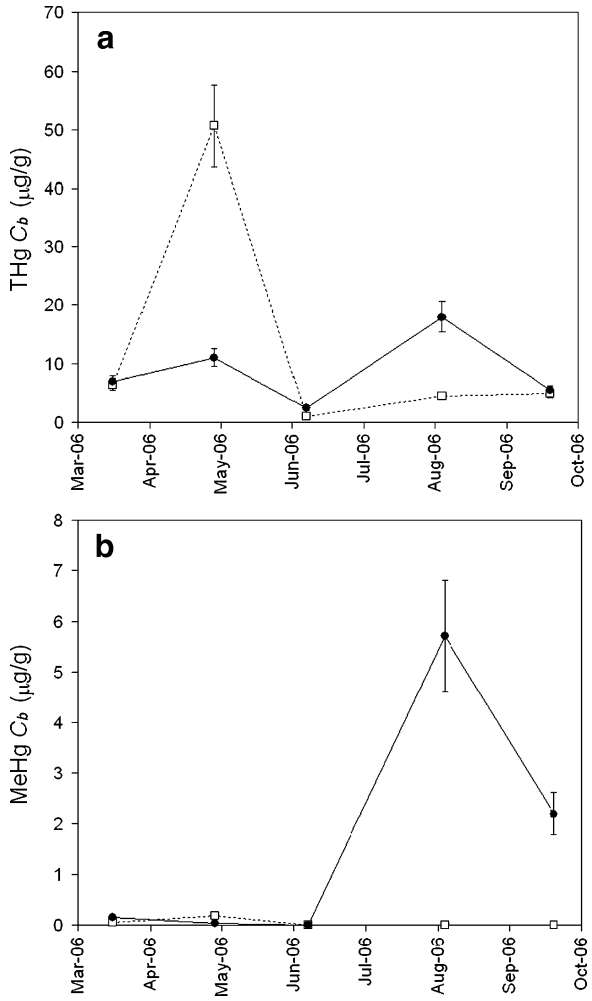

Fig. 5 Mercury concentration (C_b) in SPM <35 μm (*filled circle*) and total SPM (*unfilled square*), expressed as mercury concentration per unit mass. **a** THg C_b, **b** MeHg C_b

peak occurs when Chl*a* is comparatively low. Otherwise THg C_b for total SPM is relatively low (C_b<5 μg/g) despite a period of considerable algal growth in the late summer. THg C_b for the <35-μm size fraction shows two modest peaks: one in May (11 μg/g) and one in August (~18 μg/g). Total SPM MeHg C_b (Fig. 5b) is <0.2 μg/g in March and May and become negligible in June, August, and September, when MeHg concentrations in SPM fall below the detection limit. Seasonal MeHg C_b in the <35-μm size fraction is low during the spring runoff period (<0.2 μg/g) but increases substantially (5.7 μg/g) by August.

The partition coefficients (K_d) for THg and MeHg are presented in Fig. 6a and b, respectively. THg K_d ranges between 4.3 and 6.1 with little difference between total SPM and SPM <35 μm. THg K_d is largest in the spring when the Carson River inflows contribute large loads of suspended sediment. Spring values of MeHg K_d for total SPM and SPM <35 μm range from 4.4 to 5.0 with little distinction between the total and small size fractions. MeHg K_d then declines for both sizes in June to nearly 2.0. A similar drop in K_d is not witnessed for THg. During June, Chl*a* is at a minimum for total and small size fractions, but SPM is still high. Large drops in MeHg K_d may reflect a preferential affinity for living biomass, compared to THg which may preferentially bind to sediment. During the later portion of the summer, SPM <35 μm experiences a dramatic increase in MeHg K_d (6.6), while MeHg K_d for the total size fraction remains low. Low MeHg K_d in total SPM reflects measured concentrations below detection and illustrates the diluting nature of large, filamentous phytoplankton on the measured MeHg partition coefficient during the late summer.

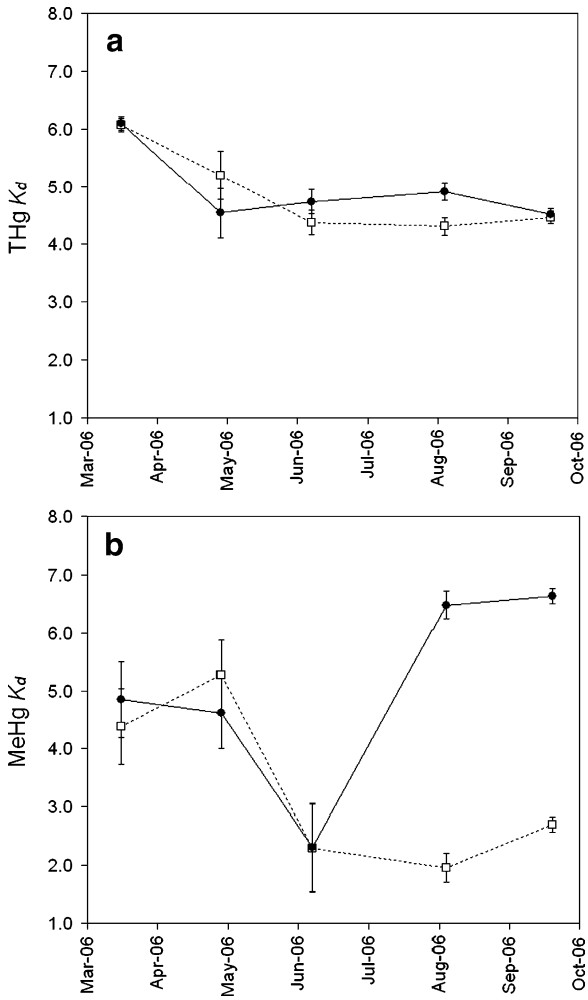

Fig. 6 Dissolved/particulate partitioning coefficient (K_d) for SPM <35 μm (*filled circle*) and total SPM (*unfilled square*). **a** THg K_d, **b** MeHg K_d

Regression analysis for C_b and K_d is performed with the following variables: Chl*a*, SPM, log-transformed W (dissolved fraction only), φ, unfiltered C_w *at Weeks Bridge,* C_w^d at FPO, and τ. Regressions are considered significant when $p \leq 0.10$, while weak relationships are considered for $p \leq 0.20$, and non-significant for $p > 0.20$. Total SPM THg C_b is found positively related to river contributions of unfiltered THg ($p < 0.02$) and not significantly related to any other variable tested. THg C_b for SPM <35 μm, showed no statistically significant relationship with any of the variables examined. Results suggest that THg at FPO is primarily associated with sediment derived from the Carson River and is not associated with phytoplankton. This affinity is biased toward larger SPM, given the lack of relationship between SPM <35 μm and unfiltered C_w at Weeks Bridge. In addition, THg C_b for smaller particles peaks when the percentage of biomass in SPM <35 μm, as well as Chl*a* (<35 μm), is increasing. However, regression analyses are not statistically conclusive. MeHg C_b in total SPM shows no relationship with tested variables, but MeHg C_b for SPM <35 μm is directly related to τ ($p = 0.02$), showing a weak positive relationship to φ ($p = 0.17$) and indirectly related to log W ($p = 0.10$) and SPM ($p = 0.06$). No relationship is found between MeHg C_b in SPM <35 μm and Chl*a*, fluvial C_w, or FPO C_w^d.

Regression analysis using K_d as the dependent variable produces similar trends to those regressions using C_b, but relationships with the partition coefficient prove statistically stronger for MeHg in SPM <35 μm. Results find THg K_d for total SPM to decrease with increased Chl*a* and increased φ, suggesting dilution by preferential sorption to sediment. However, these trends are not significant (p=0.41 and p=0.38, respectively). All other THg K_d regressions are highly non-significant. Regression analyses for MeHg K_d are provided in Fig. 7. MeHg K_d for SPM <35 μm are positively related to Chl*a* (Fig. 7a, p=0.03) and residence time (Fig. 7b, p=0.09) and negatively related to log-transformed W (Fig. 7c, p=0.06) and SPM (Fig. 7d, p=0.11). Regressions for total SPM MeHg K_d are much less significant in all cases (p>0.25) and trend in the opposite direction to the smaller fraction.

5 Discussion

Although this research generated rather small size data sets, our observations suggest that differences exist between THg and MeHg in terms of source, preferential partitioning between living and non-living SPM as well as a size dependence on partitioning efficiency.

In terms of source, observed water column concentrations confirm earlier studies that found river DMeHg contributions sufficient to explain reservoir

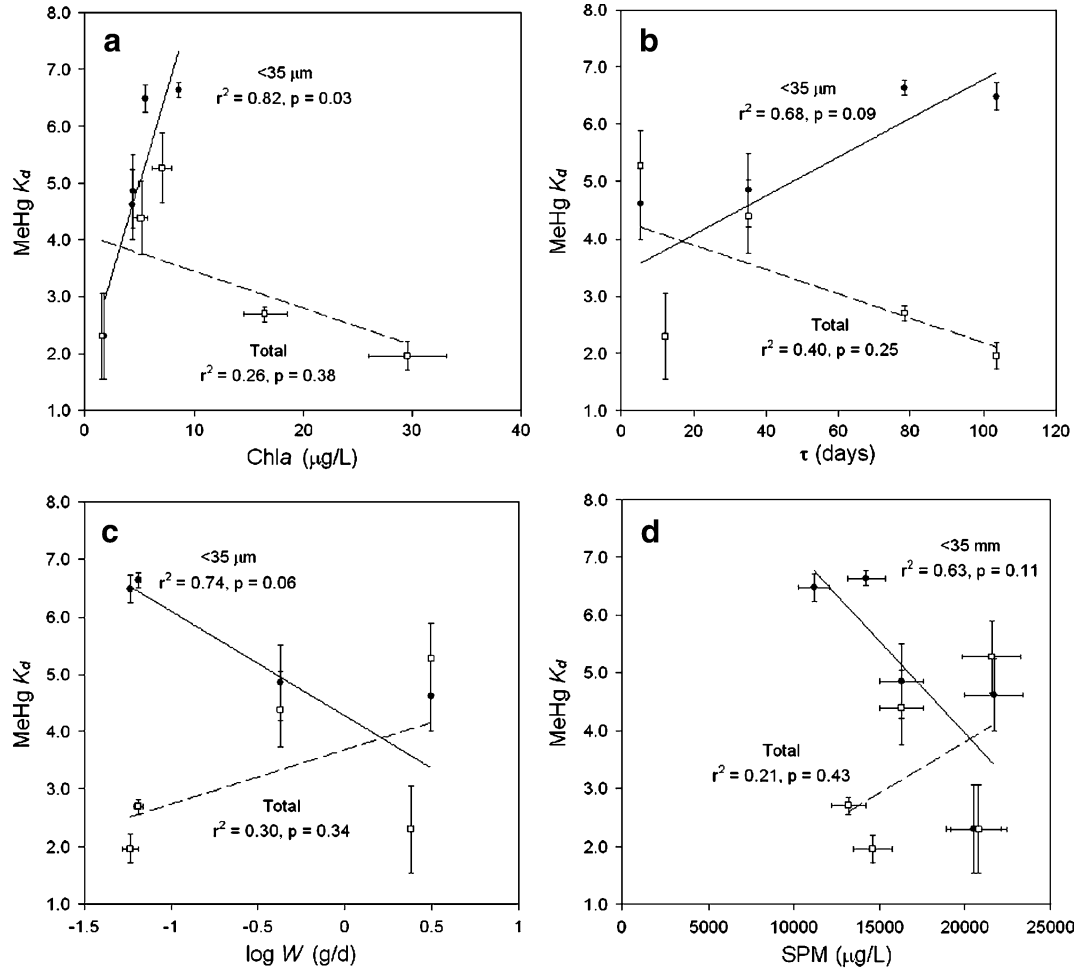

Fig. 7 MeHg K_d for SPM <35 μm (*filled circle*) and total SPM (*unfilled square*) as a function of **a** Chl*a*, **b** residence time (τ), **c** log-transformed DMeHg loads (W), and **d** SPM. Linear regression conducted on mean values with linear regression for SPM <35 μm shown as a *solid line* and for total SPM as a *dashed line*

DMeHg concentrations (Gandhi et al. 2007; Diamond et al. 2000; Hoffman and Taylor 1998; Ecology and Environment 1998). In contrast, the possibility of larger dissolved THg fluxes occurs in the south basin (Kuwabara et al. 2002), and these benthic sediments may be an important source to the reservoir. Modeling studies are underway to quantify the uncertainty associated with benthic fluxes and the relative importance of fluvial inputs into the reservoir.

In general, THg in Lahontan Reservoir is preferentially partitioned to sediment originating from the Carson River and does not appear to be a function of living biomass in the reservoir. This is evidenced by large THg concentrations associated with SPM (C_b) during the spring when THg in unfiltered water samples from the river are high, while low THg C_b are observed in the late summer when *A. flos-aquae* have large biomass. Results pertain more to particles >35 μm, since particles <35 μm produce more ambiguous results. Specifically, THg concentrations for smaller particles show tendencies to increase when small phytoplankton have net growth. THg partitioned to SPM, as defined by K_d, is similar between size fractions and remains relatively constant throughout the sampling period with no significant trend in THg K_d with respect to river loads, reservoir residence time, or biologic growth. The lack of trend in THg K_d hints that THg is a passive, sorption process that is unchanged by metabolic processes of phytoplankton. Insensitivity of THg K_d to biomass reflects preferential sorption to non-living particulates which corroborates work from other studies (Laurier et al. 2003; Schāfer et al. 2006; Pickhardt and Fisher 2007; Luengen and Flegal 2009).

MeHg appears to have a greater affinity for living biomass compared to THg as evidenced by trends in K_d, with MeHg enrichment for smaller SPM increasing with increased Chl*a*. Our results follow the trends reported by Mason et al. (1996) who found MeHg accumulation greater in living diatoms compared to dead diatoms and by Luengen and Flegal (2009) who found K_d related to factors defining algal bloom as opposed to factors related to sorption or decay. Most studies report Hg dilution with increased biomass (e.g., Pickhardt et al. 2005; Chen and Folt 2005), but work by Kirkwood et al. (1999) did find a positive correlation between concentration and biomass on a seasonal level. For the Lahontan Reservoir, the direct relationship between MeHg partition coefficient and living biomass is isolated to smaller particles. When considering the total fraction of SPM, dilution of MeHg with respect to Chl*a*, though statistically very weak (p=38), may occur. Dilution may be the result of *A. flos-aquae* large size or rapid growth rate during the late summer. Permeability of *A. flos-aquae* cell membrane is not known, nor are the *A. flos-aquae* metabolic requirements that would regulate MeHg uptake. However, both could influence the inefficiency of MeHg partitioning. Nonetheless, size distinction appears important to MeHg K_d. Lumping all sizes into a single SPM sample will skew the analysis toward low MeHg C_b and low K_d during the late summer when *A. flos-aquae* dominate the assemblage. Instead, separating out the smaller size fraction will produce different results. MeHg's possible preference for smaller, more palatable phytoplankton can have implications on systematic MeHg accumulation in Lahontan Reservoir, with implications discussed below.

Cyanobacteria are known to be a low-quality food source for zooplankton. Zooplankton growth and reproduction are inhibited by cynobacteria's filamentous structure and low digestibility (DeMott 1999; DeMott et al. 2001; Ghadouani et al. 2003). Early studies have demonstrated that cynobacteria are not readily ingested or digested by zooplankton (Hayward and Gallup 1976), and while cladocerans, such as *Daphnia pulex*, can effectively feed on single filaments of *A. flos-aquae*, they do not graze on large colonies (Holm et al. 1983). Therefore, it is assumed that any MeHg accumulation in *A. flos-aquae* acts as a temporary sink for MeHg. Upon *A. flos-aquae* death, sedimentation, and decay, MeHg can be reintroduced back into the system via the benthic community. Work in a California reservoir found that enrichment of MeHg through a benthic food web is statistically similar to enrichment in a pelagic food web, but for a given trophic position, benthic communities accumulate less MeHg than pelagic communities (Stewart et al. 2008). Low nutritional and MeHg availability from detritus, in comparison to algae and bacteria-rich diets in the pelagic zone, are offered as a reason for the difference. Therefore, if *A. flos-aquae* are found to accumulate more MeHg than more palatable phytoplankton, the benthic transfer of detrital *A. flos-aquae* MeHg would effectively reduce MeHg accumulation in top predator fish. Data from Lahontan Reservoir suggest that partitioning of MeHg to *A. flos-aquae* is minimal and that MeHg partitions

primarily in the smaller size fraction. Smaller sized phytoplankton are more readily consumed by foraging zooplankton, suggesting that the transfer of MeHg to higher trophic levels is maintained in the pelagic system. A more detailed analysis distinguishing phytoplankton biomass and SPM quality, with the inclusion of zooplankton biomass, species, and biochemical composition as well as feeding relationships (δ^{13}C and δ^{15}N) in the pelagic and benthic communities, is needed to substantiate these ideas.

6 Conclusions

Water column and phytoplankton data collected in Lahontan Reservoir are used to assess the importance of dynamic Hg loading into the reservoir as well as the importance of algal growth on the partitioning of THg and MeHg in two different SPM size fractions (total and that <35 μm). The sampling location proved turbid with THg associated with SPM explained mostly by unfiltered THg water column concentrations originating from the Carson River and not by any association with Chl*a*. The tendency for THg concentrations to decrease with increased Chl*a* helps to defend this claim. Results for THg in smaller sized SPM are less certain with statistically inconclusive but positive relationships to biomass in the water column. In contrast to THg, MeHg appears to have a stronger affinity to living biomass, with more substantial MeHg concentrations (C_b) and partition coefficients (K_d) in smaller particles during the late summer when biomass is greater and reservoir residence times longer. MeHg partitioning to smaller sized SPM, however, is lowest when loading from the river is greatest. Very different results for MeHg K_d occur if the small particle fraction is not isolated. Under these circumstances, MeHg partition coefficients are very low during algal blooms, reflecting the dilution effect of *A. flos-aquae* on the calculation. Inability of *A. flos-aquae* to accumulate MeHg may reduce the transfer of MeHg from the pelagic system to the benthic system in the form of detrital *A. flos-aquae.* Instead, small, more palatable phytoplankton appear the likely mechanism of MeHg transfer to higher trophic levels.

Acknowledgments Funding for this project came from the Nevada Institute of Water Resources Research (NIWRR) contract number 06HQGR0098. The USGS contributed federal money while the Desert Research Institute provided matching support.

References

Bloom, N. S. (1989). Determination of picogram levels of methylmercury by aqueous phase ethylation, followed by cryogenic gas chromatography with cold vapor atomic fluorescence detection. *Canadian Journal of Fisheries and Aquatic Sciences, 46*, 1131–1140.

Bonzongo, J. C., Nemer, B. W., & Lyons, W. B. (2006). Hydrologic controls on water chemistry and mercury biotransformation in a closed river system: The Carson River, Nevada. *Applied Geochemistry, 21*, 1999–2009.

Byrne, H. E., Borello, A., Bonzongo, J. C., & Mazyck, D. W. (2009). Investigations of photochemical transformations of aqueous mercury: Implications for water effluent treatment technologies. *Water Research, 43*(17), 4278–4284.

Carroll, R. W. H., Warwick, J. J., Heim, K. J., Bonzongo, J. C., Miller, J. R., & Lyons, W. B. (2000). Simulating mercury transport and fate in the Carson River, Nevada. *Ecological Modelling, 125*, 255–278.

Carroll, R., Warwick, J. J., James, A., & Miller, J. (2004). Modeling erosion and overbank deposition during extreme flood conditions on the Carson River, Nevada. *Journal of Hydrology, 297*, 1–21.

Chasar, L. C., Scudder, B. C., Stewart, A. R., Bell, A. H., & Aiken, G. R. (2009). Mercury cycling in stream ecosystems. 3. Trophic dynamics and methylmercury bioaccumulation. *Environmental Science and Technology, 43*(8), 2733–2739.

Chen, C. Y., & Folt, C. L. (2005). High plankton densities reduce mercury biomagnifications. *Environmental Science and Technology, 39*, 115–121.

Clesceri, L. S., A. E. Greenberg, & A. D. Eaton (Eds.) (1998). Standard methods for the examination of water and wastewater, 20th ed. Washington: American Public Health Association, American Water Works Association, Water Environment Federation.

Cohen, M. J., Lamsal, S., Osborne, T. Z., Bonzongo, J. C., Newman, S., & Reddy, K. R. (2009). Soil total mercury concentrations across the Greater Everglades. *Soil Science Society of America Journal, 73*(2), 675–685.

Cooper, J.J., S. Vigg, R.W. Bryce & R.L. Jacobson. (1983). Limnology of Lahontan Reservoir, Nevada: 1980–1981. Bioresources and Water Resources Centers. Desert Research Institute. DRI Publication 50021

DeMott, W. R. (1999). Foraging strategies and growth inhibition in five daphnids feeding on mixtures of a toxic cyanobacterium and a green algae. *Freshwater Biology, 42*, 263–274.

DeMott, W. R., Gulati, R. D., & Van Donk, E. (2001). Daphnia food limitation in three hypereutrophic Dutch lakes: Evidence for exclusion of large-bodied species by interfering filaments of cyanobacteria. *Limnology and Oceanography, 46*, 2054–2060.

Diamond, M., Ganapathy, M., Peterson, S., & Mach, K. (2000). Mercury dynamics in the Lahontan Reservoir, Nevada: application of the QWASI fugacity/aquivalence multispecies model. *Water, Air and Soil Pollution, 117*, 133–156.

Donkor, A. K., Bonzongo, J. C., Nartey, V. K., & Adotey, D. K. (2005). Heavy metals in sediments of the gold mining impacted Pra River basin, Ghana, West Africa. *Soil and Sediment Contamination, 14*, 479–503.

Donkor, A. K., Bonzongo, J. C., Nartey, V. K., & Adotey, D. K. (2006). Mercury in different environmental compartments of the Pra River basin, Ghana. *Science of the Total Environment, 368*, 164–176.

Ecology and Environment, Inc. (1998). Ecological risk assessment Carson River mercury site. Prepared for the U.S. Environmental Protection Agency, ARCS Region 9 and 10. ZS3490_D4700.

Gandhi, N., Bhavsar, S. P., Diamond, M. L., & Kuwabara, J. S. (2007). Development of a mercury speciation, fate and biotic uptake (Biotranspec) model: Application to Lahontan Reservoir (Nevada, USA). *Environmental Science and Technology, 26*(11), 2260–2273.

Ghadouani, A., Pinel-Alloul, B., & Prepas, E. E. (2003). Effects of experimentally induced cyanobacterial blooms on crustacean zooplankton communities. *Freshwater Biology, 48*, 363–381.

Hayward, R. S., & Gallup, D. N. (1976). Feeding, filtering and assimilation in *Daphnia schoedleri* Sars as affected by environmental conditions. *Archiv fur Hydrobiologie, 77*, 139–163.

Hoffman, R. J. & Taylor, R. L. (1998). Mercury and suspended sediment, Carson River basin, Nevada—Loads to and from Lahontan Reservoir in flood year 1997 and deposition in reservoir prior to 1983. United States Geological Survey, FS-001-98.

Holm, N. P., Ganf, G. G., & Shapiro, J. (1983). Feeding and assimilation rates for *Daphnia pulex* fed on *Aphanizomenon flos-aquae*. *Limnology and Oceanography, 28*, 677–687.

Horvat, M., Liang, L., & Bloom, N. S. (1993). Comparison of distillation with other current isolation methods for the determination of methyl mercury compounds in low level environmental samples. Part II. *Water. Analytica Chemica Acta, 282*, 153–168.

Hosseinipour, E. Z., & Martin, J. L. (1990). *RIVMOD: A one-dimensional hydrodynamic sediment transport model: Model theory and user's guide*. Athens: U.S. E.P.A.

Karimi, R., Chen, C. Y., Pickhardt, P. C., Fisher, N. S., & Folt, C. L. (2007). Stoichiometric controls of mercury dilution by growth. *Ecology, 104*(18), 7477–7482.

Kidd, K. A., Helsslein, R. H., Fudge, R. J. P., & Hallard, K. A. (1995). The influence of trophic level as measured by $\delta^{15}N$ on mercury concentrations in freshwater organisms. *Water, Air and Soil Pollution, 80*, 1011–1015.

Kirkwood, A. E., Chow-Fraser, P., & Mierle, G. (1999). Seasonal mercury levels in phytoplankton and their relationship with algal biomass in two dystrophic shield lakes. *Environmental Toxicology and Chemistry, 18*(3), 523–532.

Kuwabara, J.S., Marvin-Dipasquale, M., Praskings, W., Topping, R.R., Carter, J.L., Fend, S.V., Parchaso, R., Krabbenhoft, D.P., and Gustin, M.N. (2002). Flux of dissolved forms of mercury across the sediment–water interface in Lahontan Reservoir, Nevada. United States Geologic Survey Water-Resources Investigation Report 02-4138. U.S. Department of the Interior.

Laurier, F. J. G., Gossa, D., Gonzales, L., Breviere, E., & Sarazin, G. (2003). Mercury transformations and exchanges in a high turbidity estuary: The role of organic matter and amorphous oxyhydroxides. *Geochimica Et Cosmochimica Acta, 67*, 3329–3345.

Luengen, A. C., & Flegal, A. R. (2009). Role of phytoplankton in mercury cycling in the San Francisco Bay estuary. *Limnology and Oceanography, 54*(1), 23–40.

Mason, R. P., Reinfelder, J. R., & Morel, F. M. M. (1996). Uptake, toxicity, and trophic transfer of mercury in a coastal diatom. *Environmental Science and Technology, 30*, 1835–45.

Moye, H. A., Miles, C. J., Phlips, E. J., Sargent, B., & Merritt, K. K. (2002). Kinetics and uptake mechanisms for monomethylmercury between freshwater algae and water. *Environmental Science and Technology, 36*(6), 3550–3555.

Pickhardt, P. C., & Fisher, N. S. (2007). Accumulation and methylmercury by freshwater phytoplankton in two contrasting water bodies. *Environmental Science and Technology, 41*, 125–131.

Pickhardt, P. C., Folt, C. L., Chen, C. Y., Klaue, B., & Blum, J. D. (2005). Impacts of zooplankton composition and algal enrichment on the accumulation of mercury in an experimental freshwater food web. *Science of the Total Environment, 339*, 89–101.

Schāfer, J., Blanc, G., Audry, S., Cossa, D., & Bossy, C. (2006). Mercury in the Lot-Garonne River system (France): Sources, fluxes and anthropogenic component. *Applied Geochemistry, 21*, 515–527.

Stewart, A. R., Saiki, M. K., Kuwabara, J. S., Alpers, C. N., Marvin-DiPasquale, M., & Krabbenhoft, D. P. (2008). Influence of plankton mercury dynamics and trophic pathways on mercury concentrations of top predator fish of a mining-impacted reservoir. *Canadian Journal of Fisheries and Aquatic Science, 65*, 2351–2366.

US EPA. (1996). Method 1996: Sampling ambient water for trace metals at EPA water quality criteria levels. Washington: Office of Water Engineering and Analysis Division (4303). 20460.

Warner, K. A., Roden, E. E., & Bonzongo, J. C. (2003). Microbial Hg transformation in anoxic freshwater sediments under iron-reducing and other electron-accepting conditions. *Environmental Science and Technology, 37* (10), 2159–2165.

Warner, K. A., Bonzongo, J. C., Roden, E. E., & Ward, G. M. (2005). Effect of watershed parameters on mercury distribution in different environmental compartments in the Mobile Alabama River Basin, USA. *Science of the Total Environment, 347*, 187–207.

Warwick, J. J., & Heim, K. J. (1995). Hydrodynamic modeling of the Carson River and Lahontan Reservoir, Nevada. *Water Resources Bulletin, 31*(1), 67–77.

Watras, C. J., Back, R. C., Halvorsen, S., Hudson, R. J. M., Morrison, K. A., & Wente, S. P. (1998). Bioaccumulation of mercury in freshwater pelagic food webs. *Science of the Total Environment, 219*, 183–208.

Welschmeyer, N. A. (1994). Fluorometric analysis of chlorophyll *a* in the presence of chlorophyll *b* and pheaopigments. *Limnology and Oceanograrphy, 39*, 1985–1992.